Available online at www.sciencedirect.com

ScienceDirect

Journal of the European Ceramic Society 34 (2014) 2391–2400

www.elsevier.com/locate/jeurceramsoc

Flash-sintering of $MnCo_2O_4$ and its relation to phase stability

Anshu Gaur *, Vincenzo M. Sglavo

Department of Industrial Engineering, University of Trento, Via Mesiano 77, 38123 Trento, Italy

Received 7 November 2013; received in revised form 30 January 2014; accepted 9 February 2014
Available online 4 March 2014

Abstract

The flash-sintering behavior of manganese cobaltite spinel ($MnCo_2O_4$) is analyzed in the present work. It is shown that the $MnCo_2O_4$ is flash-sintered at 120–150 °C under 15.0–17.5 V cm^{-1}, which is substantially lower than the conventional-sintering temperatures of 1080 °C and more. We have also demonstrated that the flash-sintering is a transient phenomenon, where the power dissipation rises quickly at first and then results to Joule heating. The extent of sintering is confirmed through SEM, where a dense and pore-free morphology is observed for the well-sintered samples. The growth of secondary phase as a function of sintering temperature in both conventional and flash processes is monitored by XRD. Consistent changes in *I–V* curves observed at 200–700 °C, suggest that the rapid increase of the conductivity during flash-effect follows the hopping mechanism of usual conductivity phenomenon. On the basis of correlation between the conductivity, phase-stability and microstructure, a mechanism for flash-sintering has been proposed.

Keywords: $MnCo_2O_4$; Flash-sintering; Microstructure; Phase stability; Sintering mechanism

1. Introduction

Electric-field-assisted flash-sintering has been recently approved as a fascinating approach for achieving highly dense ceramic materials in few minutes or even few seconds. In a general description, kinetics of sintering can be enhanced by using sintering activators[1] or by incorporating external parameters such as pressure/electric field during the traditional heating.[2–4] The present work is concentrated on the latter case where the combination of temperature, pressure and electric field facilitate the mass-diffusions by lowering the (sintering) activation energy and thereby leading to the concretion of materials in shorter time. Spark plasma sintering (SPS) assisted with electric field and pressure,[2] hot pressing aided by pressure[3] and field-assisted sintering (FAS) supported by electric field[4,5] are the widely used techniques to achieve effective densification rates with reasonably lower processing conditions. In FAS electric field is employed to accelerate the densification, which result to the reduction of processing temperature by 100–150 °C; in such case the sintering time is of the same order (hours) as in conventional treatment.[4,5] Conversely, electric field assisted 'flash' sintering (FS) is unique and innovative approach which reduces the processing temperature by more than 700–800 °C, and sintering time to few minutes/seconds[4–6] relative to conventional-sintering (CS). In general, FS is accompanied with abrupt generation of charge carriers at much lower furnace temperatures, which in return cause Joule heating at resistive spots such as poorly connected grain boundaries and lattice. This effect results to sizable change in the temperature in few seconds at rates as high as 160 °C/s or more. Under such a fast change when the local temperature is reached to CS temperatures, mass-diffusions are activated and results to the densification of the samples in few minutes.[4–6] It has been shown theoretically that, with such high heating rates, reasonably very high temperature is required to produce completely dense sample.[7] Flash-sintering has been applied to a variety of materials for utilizing and understanding the phenomenon. The materials studied so far can be classified on the basis of their conductivity as insulating, like doped alumina, $SrTiO_3$,[5,8] ionic, like zirconia,[4,6] Gd-doped barium cerate,[9] electronic, like $MnCo_2O_4$[10] and, mixed ionic–electronic, like Gd-doped CeO_2[11]; apart from

* Corresponding author. Tel.: +39 0461 282468; fax: +39 0461 281977.
E-mail addresses: gauranshu20@gmail.com, anshu@ing.unitn.it (A. Gaur).

http://dx.doi.org/10.1016/j.jeurceramsoc.2014.02.012
0955-2219/

oxides, also SiC has been flash-sintered.[12] In oxides, all have tendency to increase the conductivity with temperature. Most of them are non-stoichiometric compounds (YSZ, Gd doped CeO_2, $MnCo_2O_4$, $SrTiO_3$, etc.), which form oxygen vacancies or show ionic-rearrangements. Cologna et al. has proposed possible reasons for the fast densification in FS as derived through the nucleation of defect centers (Frenkel pairs),[5] increased diffusion rate resulted via Joule heating and interaction of space charge field with the external field.[5] Narayana has proposed the defect-segregation and subsequent selective melting of grain-boundaries for increased rate of diffusions.[13] However, no direct evidence has been reported in the literature for the mechanism of defect or diffusion-site formation which gives enhanced sintering observations (to the best of author's knowledge). Thus, more measurements and studies are required in terms of conductivity, Joule heating, and defect analysis in order to construct a robust background for flash-sintering of materials. The work is intended toward understanding the cause of increased rate of densification.

Manganese cobalt oxide ($MnCo_2O_4$) is the most conductive materials with spinel structure from the family of ceramic materials that have been densified using flash-sintering.[10] The high conductivity of 60 S/cm at 800 °C[14] made this spinel suitable for application as interconnect-coating in solid oxide fuel cells (SOFC).[15,16] The purpose of using $MnCo_2O_4$ as a coating is to maintain the conductivity of the interconnect steel along with protecting it from oxidation at high temperature[15] and the cell from Cr-poisoning.[17,18] The SOFC demands dense coating for interconnects which should not possess open porosity. On the other hand, $MnCo_2O_4$ sintering demands high temperatures of 850–1300 °C[18] which are not desirable for Crofer steel. Several hours of sintering at low temperature are responsible for the growth of chromia layer, which increases the resistance of the stack.[16] Flash-sintering is a promising approach in such temperature sensitive application for its 'very low time and lower temperature' demand. Prette et al. have reported the possibility of flash-sintering on Mn–Co oxide in bulk form.[10] In such study, ceramic oxide has been field-treated without current control and this produced very high power dissipation. It is not clear if such high values are the necessary requirement for sintering. Moreover, the unusual fastness in temperature-increase during flash-sintering can cause the mechanical fracture of the ceramic specimen. Therefore, the minimum of parameters (power dissipation in terms of electric field and current density) are required to estimate in order to better control the processing of spinel oxide. The other issue with the sintering of $MnCo_2O_4$ is related to its phase stability at high temperature.[19] CS leads to the formation of secondary phases which subsequently results in a decreased conductivity.[19] Thereby, it diminishes the role of $MnCo_2O_4$ which is preferably used for its higher conductivity in SOFC and as a conducting phase for mixed ionic-electronically conductive (MIEC) application.[16,19] Because of this reason, in practical applications, an optimal value for sintering temperature and time are chosen in order to achieve the desired mechanical and conductive properties.[19] The drastically reduced time and lower temperatures features of FS are expected to be helpful to obtain the desired spinel phase structure of $MnCo_2O_4$. Moreover, it will also be useful to analyze the correlation between sintering and stability of spinel phase during FS.

The purpose of the present study is to understand the flash-sintering behavior of $MnCo_2O_4$ spinel and to deal with the issues involved with high temperature conventional treatments. For this, microstructure and phase composition changes are analyzed in terms of the local temperature and are correlated with the results of conventional-sintering. Conductivity and Joule heating property of the spinel are discussed to further investigate the flash-effect. On the basis of the results we made an attempt to understand the mechanisms involved in the flash-sintering of the spinel.

2. Materials and methods

Commercial $MnCo_2O_4$ powder (average particle size ~1.17 μm, surface area = 4.22 g/cm^2) was mixed homogeneously with 3 wt% Duramax B-1000 binder and pressed uni-axially into dog-bone shaped samples. These samples were pre-sintered at 900 °C for 1 h in order to remove binder and to allow easier handling for successive flash-sintering experiments. Sintering was performed by four-point electrical arrangements using platinum wires in a furnace which was heated with a constant rate of 5 °C/min. Gauge section was 20 mm long with cross section of (1.65 ± 0.05) × 3.0 mm^2. Conducting LSC (lanthanum strontium cobaltite) slurry and silver paste were used to reduce the contact resistance. The voltage was applied using Sorensen XG6025 power supply; the voltage drop across the sample was measured using Keithley 2100 digital multimeter; the current through the circuit was measured by recording the voltage across a shunt of 0.002 Ω using Keithley 2000 digital multimeter. Flash-sintering experiments were performed by applying different DC electrical fields (2.5–17.5 V cm^{-1}); current was set to a fixed value providing maximum density of 1.40–1.60 A/mm^2 with the aim to avoid any kind of thermal/electrical runway in the sample to protect the connecting Pt wires and the sample from excessive heating; all the voltages were applied from starting furnace temperature of ~100 °C; samples were kept on hold for 60 s at the maximum values. Specimen temperature was recorded using a pyrometer (Ultimax Infrared Thermometer, UX-20/600–3000 °C) in the similar experimental arrangement. Prior to the measurements, pyrometer was calibrated for the spinel up to 1150 °C (with no field applied). Sampling rate for data recording in pyrometric and power dissipation measurement was approximately 0.17–0.20 s. Microstructural characterization was carried out by JEOL JSM-5500 SEM (scanning electron microscope). Phase composition analysis was performed using Rigaku X-ray diffractometer (using Cu Kα radiation). *I–V* characteristics were recorded at constant furnace temperature in the range of 200–700 °C. The field was increased with a rate of 8 mV cm^{-1} s^{-1} up to approximately 7.0 V cm^{-1}. Thermo-gravimetry was performed at different heating rates by NETZSCH Gerätebau STA 409 Thermo-balance.

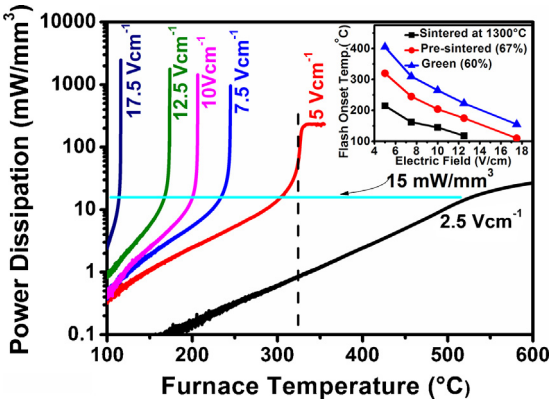

Fig. 1. Power dissipation in 67%-dense pre-sintered $MnCo_2O_4$ samples as a function of furnace temperature under different applied electric fields. Variation of flash onset furnace-temperature with electric field for different density samples (Green-60%, Pre-sintered-67% and sintered at 1300 °C) is shown in the inset.

3. Results

3.1. Flash sintering

The variation of power dissipation as a function of furnace temperature at different applied electrical fields on 67%-dense pre-sintered $MnCo_2O_4$ dog bone shaped sample are presented in Fig. 1; power dissipation is calculated from the product of applied electric field and the current density through the sample. It is clearly shown that the electric field has strong influence on the power dissipation behavior of the sample. At relatively low applied field (2.5 V cm^{-1}) the power dissipation shows almost linear dependence on the furnace temperature up to 550 °C, which is the usual conductivity behavior of $MnCo_2O_4$. For fields greater than 5 V cm^{-1} the linear dependence occurs with slightly higher slopes up to an onset temperature beyond which a sudden rise in power dissipation is observed. This sudden rise in the power dissipation curve is the sign of flash-sintering.[4,10] From Fig. 1, it is observed that the initiation of such flash-sintering behavior for $MnCo_2O_4$ is commenced under 5 V cm^{-1} and 320 °C threshold field and threshold furnace temperature, respectively. At further higher applied fields, the dissipation plots show similar sudden increase behavior (represented by vertical line, flash effect) at ∼15 mW/mm^3. These observations are in agreement with previous works on $MnCo_2O_4$ where threshold furnace temperature is at 475 °C[10]. The deviation of threshold temperature from the reported literature[10] by ∼155 °C is expected to be due to the difference in the initial density of the samples. As a matter of fact, flash-effect depends on the conductivity of the material and it is described by the combination of electric field and temperature[4]; the density of the sample has therefore a significant role on flash-parameters. The variation of onset furnace temperature as a function of electric field for different density samples (green: 60%, pre-sintered: 67%, sintered at 1300 °C: full density) is presented in the inset of Fig. 1. The abrupt change that occurs during flash-sintering is observed in all samples, whether it is tightly packed sintered or loosely held green sample. According to such observation and previous works,[7,20] the flash-effect of rapid increase in conductivity and quick sintering is suggested to be an intrinsic property of the material, not simply connected to resistive heating at particle–particle contacts in the green sample (during rapid increase of current); equally it is evident in dense samples also. In other words, it is proposed that every material could show specific flash-effect.

Samples with different densities show the same threshold field of about 5 V cm^{-1}; but the onset temperatures at the same applied field changes with the density of the samples. The onset temperature difference of about 120 °C between green and fully dense sample was observed at 10 V cm^{-1}. In general, the conductivity of the materials is a coupled response of bulk of the particle and inter-particle connectivity in the sample.[21,22] The constant threshold field observed for different density samples suggests that the conductivity of the spinel dominantly comes from the bulk properties and even a small channel through particle-particle connection can provide such conductivity that does not significantly affect the flash-parameter. On the other hand, the deviation in the onset temperatures is expected to be associated to the difference in the inter-particle connectivity in the samples. Similar observation on the conductivity of $MnCo_2O_4$ has been previously reported where inter-particle connections lead to enhanced conductivity of the material.[19] The pre-sintered sample with 67% density, shown in the inset of Fig. 1, shows flash-sintering at much lower furnace temperatures, at about 120–250 °C, under 7.5–17.5 V cm^{-1} field; the sintering temperature is therefore 1000–1100 °C lower than conventional heat treatment requirement of 1300 °C. From this result we propose that $MnCo_2O_4$ material can be sintered by the flash-effect at 120–250 °C without the requirement of high electric fields.

The evolution of the 67%-dense pre-sintered sample under flash-sintering is here analyzed.

The specimen temperature (T_s) measured by pyrometer during flash-sintering, along with the details of the applied field and power dissipation across the samples, is reported in Table 1. The amount of power dissipation observed for $MnCo_2O_4$ spinel reported in Fig. 1 as well as in the table is substantially high compared to those required for the flash-sintering of other low-conductive materials.[4,5,8] Further, increase of 50–75 °C in specimen temperature involves with 250–300 mW/mm^3 increase in power dissipation. Such high power dissipation values are directly related to the low activation energy and higher conductivity of $MnCo_2O_4$. The change in specimen temperature (dotted line) during flash-sintering as a function of time for the 67%-dense pre-sintered $MnCo_2O_4$ sample under the electric field of 10 V cm^{-1} is presented in Fig. 2. The variation of power dissipation (solid line) with time is also included in the same figure in order to correlate the two behaviors. The power dissipation curve is the magnified part of 10 V cm^{-1} curve presented in Fig. 1 (pink line) and is shown to have anomalous effect at 210 °C furnace temperature. A sudden increase in power dissipation from a minimum of 15 mW/mm^3 to a maximum of 1445 mW/mm^3 is observed within a short interval of time (∼5 s). Afterwards drop in the power dissipation is due to the maximum

Table 1
Specimen temperature with corresponding electric field and power dissipation measured in the flash-sintering experiment.

Sample name[a]	Furnace temperature (°C)	Electric field (V cm^{-1})	Maximum current density (A/mm^2)	Maximum power dissipation (mW/mm^3) (V = 95–99 mm^3)	Specimen temperature (°C)
–	320	5.0	0.48 (material's limit)	240	<900
FS925	250	7.5	1.25 (material's limit)	960	925
FS975	210	10.0	1.40	1445	975
FS1050	170	12.5	1.40	1800	1050
FS1100	145	15.0	1.40	2160	1100
FS1160	120	17.5	1.40	2475	1160
FS1320	120	17.5	1.60	2830	1320

[a] Sample name: FS stands for flash-sintered, followed with local (specimen) temperature recorded using pyrometer.

current limit specified in the measurement set up, where the power supply switches from constant voltage to constant current control. The decrease in the power dissipation in such constant current region is a sign of conductivity increase.[7] After the power dissipation decrease, a steady state value is reached at longer hold time, indicating the saturation of conductivity through the sample. The specimen temperature which occurs as a consequence of power dissipation, exhibits the similar sharp increase with time. The specimen temperature shows a rapid increase up to ~975 °C under 10 V cm^{-1} just after the increase of power dissipation. Such increase in the specimen temperature is the outcome of Joule effect, occurred for large increase in the conductivity at very low furnace temperature (210 °C). The observation is manifested in the time lag (~2–3 s) between the two curves, where the specimen temperature follows the power dissipation trend. Under such change, specimen achieves the maximum temperature in the stabilization region, just before the steady state power dissipation. This increase in local temperature facilitates the flash-sintering of the sample. At higher applied fields, relatively higher local temperature is achieved in the same time interval, which involves comparatively more drastic changes in power dissipation and specimen temperature (Table 1). Similar observation of flash-sintering during the stabilization of power dissipation, in the short time interval between the peak and the constant value, is reported for zirconia.[7]

The extent of sintering was analyzed by the SEM for the samples subjected to various applied fields. The micrographs

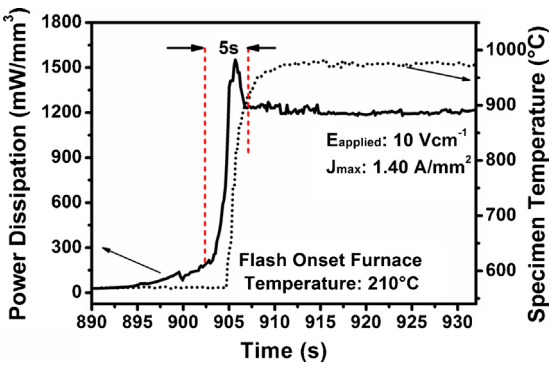

Fig. 2. Power dissipation and specimen temperature as functions of time for sample FS975, flash-sintered under 10 V cm^{-1}.

of 67%-dense pre-sintered $MnCo_2O_4$ sample subjected to different applied electric field (7.5–17.5 V cm^{-1}) which in return produces different local temperatures are shown in Fig. 3. The details of field applied, furnace temperature and power dissipation are provided in Table 1. The microstructure of conventionally sintered (CS) samples at similar temperatures is also compared. In this case, the furnace temperature is considered as the specimen temperature. The CS samples are sintered with a heating rate of 5 °C/min, with hold time of 60 s and furnace temperature is measured by keeping the furnace thermocouple close to the sample surface for attaining the good correlation with FS samples. Samples are here labeled with prefix FS for flash-sintered and CS for conventionally sintered, followed by the specimen temperature (Table 1). The microstructure of FS925 sample (Fig. 3(b)) shows close resemblance with that of pre-sintered sample in Fig. 3(a), which suggests that the microstructure is not affected by the flash-effect observed at such low field and the specimen temperature. The microstructure of FS975 specimen (Fig. 3(c)) shows that an incipient grain growth, which is well pronounced in FS1050 sample (Fig. 3(d)). The grain growth is preferentially unidirectional and isolated small grain appears together with elongated grains. The grain morphology of CS sample sintered at 1050 °C (Fig. 3(e)) exactly replicates that of FS1050 (Fig. 3(d)). Nevertheless, the extent of porosity estimated by image-binarisation[23] using MATLAB software suggests that the FS sample has comparatively higher porous nature. The higher porosity in FS samples is expected to be associated to unidirectional grain growth and flash-sintering effect. At higher temperature, a sudden change in the morphology is observed for FS1100 (Fig. 3(f)): the micrograph shows that the grains are substantially larger and grain to grain connections are developed with reduced porosity. The CS1100 sample (Fig. 3(g)) shows poor morphology with lower grain size and higher porosity compared to its counterpart of FS1100 (Fig. 3(f)). Similar observations are found for further higher sintered samples. A fully connected grain structure with average grain size of about ~8 μm and without open porosity is observed for FS1160 sample (Fig. 3(h)). The CS sample produced at the same temperature (1160 °C) possesses smaller grains with average grain size of ~5 μm (Fig. 3(i)). The morphology of FS sample sintered at 1320 °C (Fig. 3(j)) shows melted-like appearance without clear visibility of grain boundary in contrast to

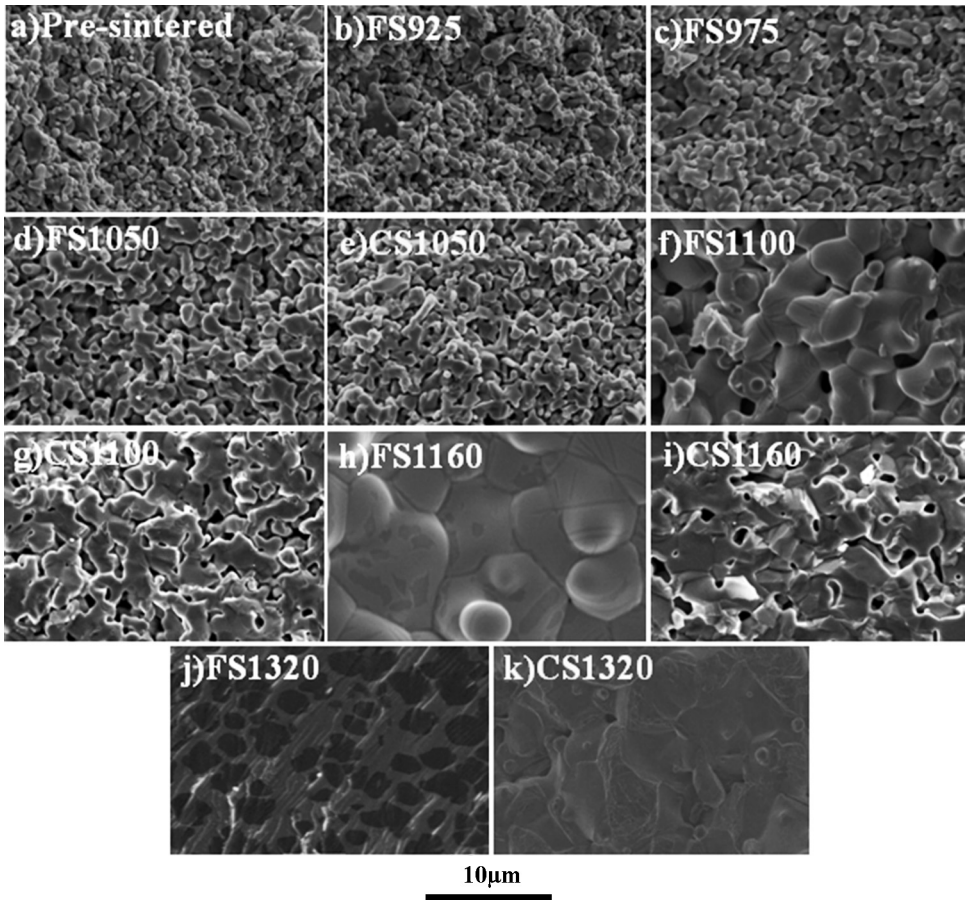

Fig. 3. SEM micrograph of (a) pre-sintered, flash-sintered sample namely (b) FS925, (c) 975, (d) FS1050, (f) FS1100, (h) FS1160 and (j) FS1320, and conventionally sintered samples, (e) CS1050, (g) CS1100, (i) CS1160 and (k) CS1320 presented for comparison. FS samples are produced under 7.5–17.5 V cm^{-1} at furnace temperatures of 120–250 °C.

large grains of CS1320 (Fig. 3(k)). Black spots in Fig. 3(j) represent regions with higher Co concentration as detected by EDS; such regions originate from the reduction of $MnCo_2O_4$ to CoO[19] which will be discussed in the next section.

From SEM analysis, we conclude that the electric field sintering has a strong effect on the microstructure of the specimen at high temperatures. The FS sample microstructure sintered at lower temperatures (up to 1000–1050 °C) has close resemblance with that of its counterpart of CS with slight change in the porosity. It is inferred that the strong flash-effect and fast change in specimen temperature (Fig. 2) is not the only requirement for the flash-sintering (with additional sintering over CS) of $MnCo_2O_4$. However, a fully dense morphology with interconnected grain structure is observed at higher temperature (in excess of 1100 °C). This observation is dissimilar to that made on FS zirconia, where a relatively higher shrinkage is reported over the conventional sintering at temperatures from 950 to 1600 °C.[24] In addition, $MnCo_2O_4$ forms relatively larger grains in flash-sintering, which is again dissimilar from previous findings on zirconia[4] and $SrTiO_3$[8] where similar and smaller grain size, respectively, is reported under flash-sintering. Flash-sintering was previously thought to inhibit grain growth due to lower processing time (and temperature) but from the results obtained on $MnCo_2O_4$ this cannot be a general statement.

The phase composition of 67%-dense pre-sintered $MnCo_2O_4$ sample under FS and CS at different temperature was analyzed by X-ray diffraction (XRD). The XRD patterns are shown in Fig. 4. The XRD pattern of FS975 sample (Fig. 4(a)) shows sharp diffraction pattern which exactly coincides with that of the raw powder. The XRD pattern was identified as belonging to the cubic spinel phase of $MnCo_2O_4$ (JCPDS File No: 023-1237). The spinel diffraction pattern is well preserved at higher sintering temperatures up to 1050 °C, i.e. in FS975 and FS1050, respectively. At further higher sintering temperatures, a sharp peak centered around $2\theta = 42.01°$ and a small peak appearing as right shoulder of the (3 1 1) reflection of $MnCo_2O_4$ phase are observed. These new set of peaks are identified as belonging to the face centered cubic structure of CoO according to JCPDS file No: 065-2902. The intensity of the CoO phase pattern is observed to increase with sintering temperature along with the suppression of original $MnCo_2O_4$ phase pattern. In general, the intensities ratio of the two different phases is proportional to the weight fraction of the substances[25,26]:

$$\frac{I_{CoO}}{I_{MnCo_2O_4}} = \frac{w_{CoO}}{w_{MnCo_2O_4}} \quad (1)$$

where $I_{MnCo_2O_4}$ and I_{CoO} are the intensity of strong XRD reflection of $MnCo_2O_4$ and CoO, respectively, while $w_{MnCo_2O_4}$ and

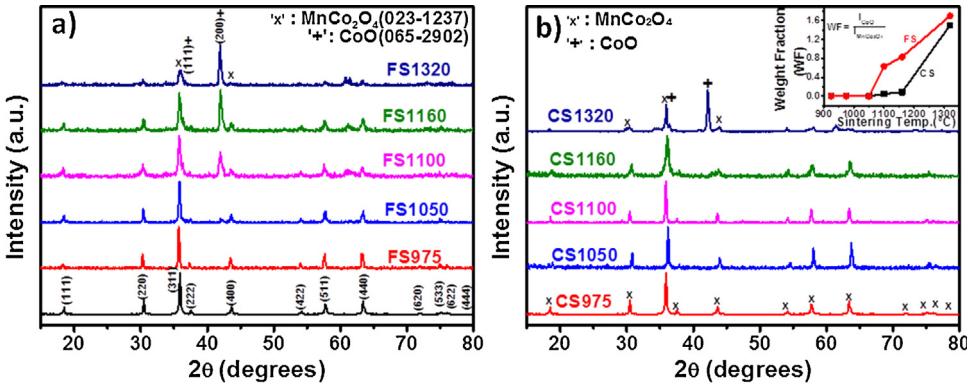

Fig. 4. XRD of flash-sintered samples namely (a) FS975, FS1050, FS1100, FS1150 and FS1320 along with as-observed $MnCo_2O_4$ powder, and conventionally sintered samples (b) CS975, CS1050, CS1100, CS1160 and CS1320. The weight fraction of CoO and $MnCo_2O_4$ for flash and conventionally sintered samples as functions is given in the inset of (b).

w_{CoO} are the weight fractions of $MnCo_2O_4$ and CoO, respectively. The ratio of the area (integrated intensity) under the strong peaks of (2 0 0) CoO and (3 1 1) $MnCo_2O_4$ is calculated and its variation as function of specimen temperature is shown in the inset of Fig. 4(b). The (3 1 1) reflection of $MnCo_2O_4$ at $2\theta = 36°$ shows a right shoulder at $2\theta = 36.5°$ of (1 1 1) reflection of CoO phase. The strong peak at $2\theta = 36°$ is de-convoluted into two peaks centered at 36° and 36.5° and then the area under the (3 1 1) peak is evaluated. The increase in the intensity ratio is a measure of the growth of CoO or of the suppression of $MnCo_2O_4$. The inset in the Fig. 4(b) shows a systematic increasing trend of the intensity ratio with the temperature above 1050 °C. This is also evident from the peak intensities variation in Fig. 4(a). Conversely, CS samples are mono-phasic up to much higher temperatures. The set of XRD diffraction pattern presented in Fig. 4(b) for CS samples shows that the single phase of $MnCo_2O_4$ is preserved up to 1100 °C. A weak CoO pattern is observed for CS1160 sample, whose intensity increases for higher sintering temperature as in sample CS1320. The ratio of the peak intensity presented in the inset of Fig. 4(b) shows that the curve deviates from its counterpart of FS samples. The FS samples show sudden increase in the peak intensity ratio at 1100 °C. A comparison between FS and CS spectra shows greatly enhanced cobalt oxide peaks intensity for FS samples. The two treatments (FS and CS) are performed for the same sintering time of 60 s with CS at the heating rate of 5 °C/min and FS at 9600 °C/min (160 °C/s) or more. From XRD study we conclude that the spinel phase is stable up to specimen temperatures of 1050 °C in flash-sintering and 1160 °C in conventional-sintering. Both conventional-sintering and electric field assisted flash-sintering show the formation of secondary phase at higher specimen temperatures. However, the flash-sintering shows CoO phase concentration higher than its counterpart at all corresponding sintering temperatures. The observations from XRD are found in correlation with SEM results where flash-sintering is found to enhance over conventional at temperatures of 1100 °C and higher. From this study we conclude that the microstructural-growth and phase-decomposition are shared processes and the sintering might have derived through the actions involved in the phase decomposition.

4. Conductivity of $MnCo_2O_4$ spinel

Flash-sintering phenomenon starts with an abrupt increase in conductivity (flash-effect), subsequent Joule heating followed by mass-diffusions and eventually leading to sintering. To investigate the details of flash-effect in $MnCo_2O_4$, we carried out electrical conductivity and *I–V* measurements on sintered samples. The conductivity of $MnCo_2O_4$ spinel sintered at 1050 °C and 1300 °C for 2 h was measured in an experimental arrangement similar to that used for flash-sintering and the results are compared in Fig. 5. The samples are subjected to sintering to avoid stimulated effects due to dimensional-changes and porosity. From Fig. 5, one can observe that the conductivity of both samples increases with temperature. In addition, the conductivity is lower for the sample sintered at higher temperature of 1300 °C with no appreciable change in the semiconducting behavior. The decrease in the conductivity is expected to be due to the formation of low-conductive secondary CoO phase[27] as it is clear from the XRD analysis. Yi et al. reported the growth of similar low conductive phase when $MnCo_2O_4$ is sintered at higher temperature.[19] The conductivity of $MnCo_2O_4$ sample sintered at 1300 °C (Fig. 5) is lower than that reported in previous works on Mn-Co oxide,[14,19] this probably being related to contact resistance and different experimental arrangement. However, in the present investigation, we are interested on the

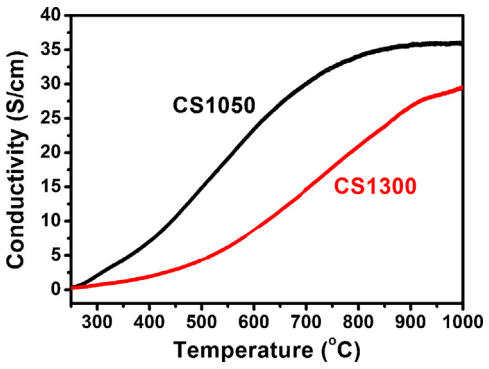

Fig. 5. Electrical conductivity of $MnCo_2O_4$ samples sintered at 1050 °C and 1300 °C for 2 h as a function of temperature.

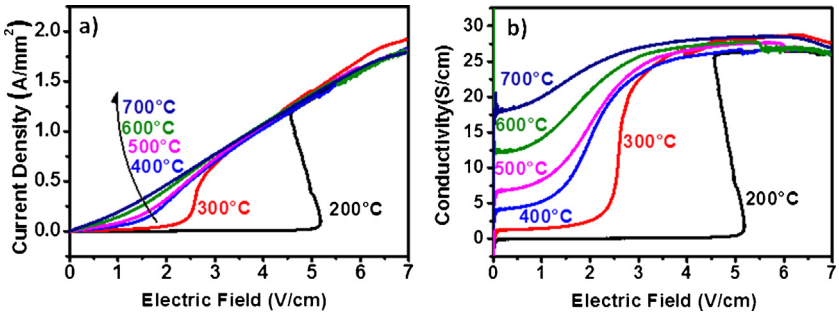

Fig. 6. *I–V* characteristics of $MnCo_2O_4$, sintered at 1300 °C, recorded at different furnace temperatures from 200 to 700 °C, presented as (a) current density as a function of electric field, (b) conductivity as a function of electric field.

variation of conductivity with temperature. With the observation that the high temperature sintering does not affect the conductivity behavior of $MnCo_2O_4$, we carried out current–voltage measurements on fully dense $MnCo_2O_4$ samples sintered at 1300 °C.

Current–voltage (*I–V*) characteristics of 1300 °C pre-sintered $MnCo_2O_4$ samples measured at different furnace temperatures (200–700 °C) are compared in Fig. 6(a). The electric field is applied at an increasing rate of ~8 mV cm^{-1} s^{-1}. From the curve it is observed that the furnace temperature has significant effect on the *I–V* curve of $MnCo_2O_4$ sample. At 200 °C, the current grows linearly up to 5.18 V cm^{-1} but with very small current density compared to that recorded at other temperatures. As the field reaches 5.18 V cm^{-1}, the current increases at faster rate with the appearance of flash-like-effect. The increasing rate of the current was so fast that at the same time the field decreased down showing backward flow in the *I–V* characteristics. A comparison with the inset in Fig. 1 for the sample sintered at 1300 °C suggests that there is a close match between the temperature and field values for flash-effect, (210 °C, 5 V cm^{-1}) and (200 °C, 5.18 V cm^{-1}), where one measurement is performed in constant-field experiment and the other at constant-temperature. This represents the consistency of flash-effect, and invariability of the material's property to respond under the electric field. Fig. 6(a) shows that the flash characteristic nature of $MnCo_2O_4$ in *I–V* curve gradually reduces to smooth behavior at higher temperatures. For temperature of 300 °C, the current shows a linear dependence on the voltage with slightly higher slope and a sudden increase at 2.1 V cm^{-1}, which is much earlier than at 200 °C. However, the extent of current density increase at flash-effect field is relatively lower than that obtained at 200 °C. At further higher furnace temperature, such flash effect is not observed and the *I–V* behavior is almost linear at 400–700 °C temperatures with a not-significant non-linearity (in 1–2 V cm^{-1} field range). A similar observation is recorded from the inset in Fig. 1, where furnace temperatures higher than 200 °C belong to the FAST regime, the material showing a smooth current increase. For all furnace temperatures, after the non-linear changes (either strong or moderate) the current increases linearly with the field. The variation in the conductivity of $MnCo_2O_4$ samples pre-sintered at 1300 °C as a function of the applied electric field is shown in Fig. 6(b). The flash-effect corresponding to increased conductivity is clear. The conductivity reflects the same trend of *I–V* curve (Fig. 6a) and shows flash-like abrupt behavior at 200 °C. It can be observed that the conductivity increases in a non-linear manner with the applied field at all temperatures. However, the non-linearity feature varies with the furnace temperature. At 200 °C, the conductivity is almost constant until a critical field is reached, at which the spinel undergoes to a strong non-linear increase (flash-effect). For temperatures in excess of 200 °C, the non-linear feature is comparatively modest but starts occurring from initial field-values. All graphs show a systematic change from strong to moderate non-linear behavior from 200 to 700 °C. Under different degree of non-linearity with the electric field, all curves seem to reach a common stable value.

The discussions on the conductivity and flash-effect are extended considering the measurement of specimen temperature. The variation of specimen temperature (solid line) and current density (dotted line) with electric field for $MnCo_2O_4$ sample recorded at different furnace temperatures are presented as functions of time in Fig. 7. Both, the specimen temperature and current density are correlated to each other and are observed to follow abrupt and gradual changes with time at 200 °C and 600 °C furnace temperature, respectively (Fig. 7(a)). At 200 °C furnace temperature, the specimen temperature raises abruptly to more than 900 °C following the trend of the current density and increases continuously with the applied field beyond the flash effect. The changes are comparatively smoother at furnace temperature of 600 °C; in any case, the specimen temperature rises above the furnace temperature by Joule heating. Close observation of 200 °C curve in the inset of Fig. 7(a) suggests that it is the increase in conductivity which drives the Joule effect (also evident in Fig. 2). This observation is not so clear at 600 °C because of comparatively smooth variations of current and specimen temperature. For the case of 300 and 400 °C furnace temperatures in Fig. 7(b) which belong to the FAST regime, we observe the same sign of flash-effect-controlled-Joule heating which is clearly visible in 200 °C case. Thus, for the considered field range, the spinel attributes increase in conductivity, thereby Joule effect at lower as well as higher temperatures, though in different extent. These fields are sufficient to interact with $MnCo_2O_4$ system for increasing the conductivity and further resulting to Joule heating.

From the quantitative comparison of the conductivity values in Figs. 5 and 6(b), one can derive interesting correlation between the intrinsic conductivity and flash-effect. The conductivity behavior at each temperature resembles the (non-linear) conductivity curve of Fig. 5. In addition, at each temperature in Fig. 6(b),

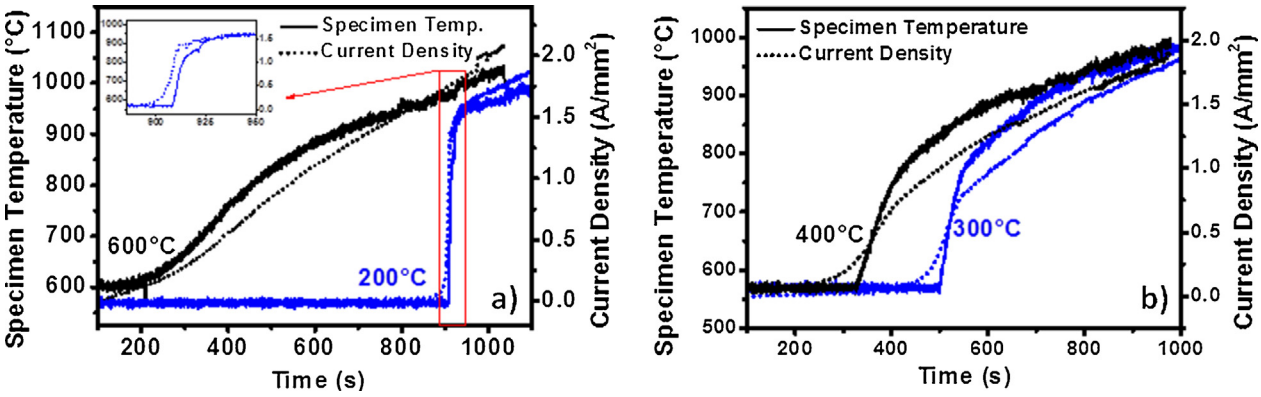

Fig. 7. Current density and specimen temperature of $MnCo_2O_4$ samples sintered at 1300 °C as functions of time recorded at (a) 200 and 600 °C, (b) 300 and 400 °C.

the initial conductivity represents the value derived purely from thermal effects and it matches closely with the observations recorded in conductivity measurement in Fig. 5. Further, approximately the same conductivity of 27.5–28.7 S/cm, corresponding to the constant value after strong or modest flash-like-effect in Fig. 6(b), is recorded in the measurements reported in Fig. 5 at ~1000 °C (29.5 S/cm). Fig. 7 suggests that the specimen temperature during such flash effect is approximately 1000 °C and therefore in both cases similar specimen temperature of about 1000 °C is attained. Here, it is worth mentioning that conductivities shown in Fig. 5 are purely based on thermal effects, whereas in Fig. 6(b) it is assisted with the additional effects of electric field. From this observation we suggest that the conductivity behavior under electric field follows similar mechanism involved in conventional measurement (with weak field). In both cases, the increase in conductivity is associated with the generation of new current carriers. The increasing rate of the carriers depends on the temperature in constant field experiment and on the applied electric field in the constant temperature experiment. On the basis of presented results, we made an attempt to understand the mechanism involved in the generation of charge carriers which eventually leads to higher conductivity in the spinel oxide.

5. Discussion

The conductivity of $MnCo_2O_4$ spinel is reported to follow polaron hopping mechanism[19,28] and is governed by the hopping of oxidation states between Co^{3+}/Co^{2+} and Mn^{4+}/Mn^{3+} pairs.[28,29] These hopping states are bidirectional and are responsible for the relatively high conductivity of the spinel. Transitions related to cobalt states are described as

Forward transition :

$$Co^{3+} \xrightarrow{\text{thermally activated}} Co^{2+} + 1 \quad \text{oxygen site} \tag{2a}$$

Backward transition :

$$Co^{2+} \xrightarrow{\text{non-radiative loss of energy}} Co^{3+} + \text{loss of} \quad 1 \quad \text{oxygen site} \tag{2b}$$

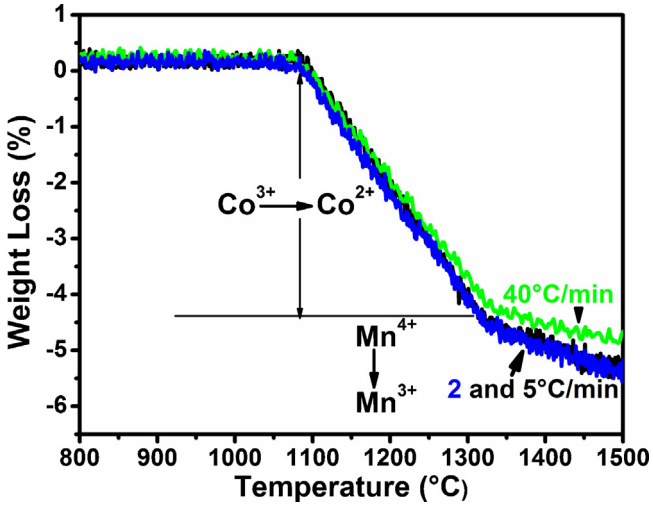

Fig. 8. Weight loss as a function of temperature for $MnCo_2O_4$ at three different heating rates, 2, 5 and 40 °C/min.

These transitions are thermally activated.[30,31] As temperature increases, the number of such transition also increases and therefore the conductivity becomes higher.[30,31] At higher temperatures, the hopping transition occurs more frequently in one direction and hence the conductivity increase becomes slower. As a consequence, the weight loss corresponding to oxygen deficiency takes place and this behavior is well observed in thermo-gravimetry (TG) analysis.[29] The TG response of $MnCo_2O_4$ spinel is shown in Fig. 8, the measurements having been made at three different heating rates, 2, 5 and 40 °C/min. TG curve shows a two-step weight loss; the first at 1080–1320 °C, the second between 1320 °C and above 1500 °C. The first weight loss corresponds to Co^{3+}/Co^{2+} while the second is associated to Mn^{4+}/Mn^{3+}.[29] It is observed that the onset temperature for each weight loss is independent from heating rates; however, the extent of weight loss decreases at higher heating rates. On the basis of this observation, we expect that the same onset temperature and weight loss decrease take place during high heating rates of flash-sintering. It is interesting to correlate the observations drawn from TG curve with that of the Co-oxide phase recorded in XRD analysis (Fig. 4(b)). The CS samples heat treated up to 1050 °C do not show Co-oxide phase, but at higher temperatures

there is an increasing formation of CoO. These weight loss and phase structure are reported to be reversible and can be achieved back if cooling rate is very slow (2 °C/min or less).[29] However, at fast heating/cooling rates as in FS samples, the possibility of retaining the transformations decreases. Therefore, the weight loss and the CoO phase formations remain in the sample after the flash-effect. This is well evident from the XRD analysis of FS samples, where the prominent CoO phase is observed much earlier than CS samples.

Moreover, the hopping mechanism leads to the formation and annihilation of ionic-sites as discussed in Eq. (2) which are expected to be used for mass-diffusion. In the context of sintering, there is the possibility of two effects to occur with such exploitable sites: (1) backward transition Co^{2+}–Co^{3+} which reduces the generated ionic-sites and (2) maintenance of the Co^{2+} state which increases the life of O-site. The TG and XRD analyses suggest that these effects depend on the sintering temperature. At temperatures below 1080 °C, the two transitions are equally probable and there will be no ionic-sites available for mass diffusion; this state is unfavorable for sintering to occur. As a consequence to equal probability, no weight loss and no Co-oxide are detected in TG and XRD study respectively. At temperature higher than 1080 °C, the formation of ionic-sites is more favored than its counterpart of annihilation which gives rise to weight loss and phase separation. The lower probability for backward transition increases the life of ionic-sites (Eq. (2)) which in return facilitates the mass diffusion and eventually leads to the sintering. The transition related to Mn is not discussed here as it falls out of the sintering temperature range for spinels (Fig. 8). By extending the ideas drawn from conventional sintering and the results observed in our present work, we made an attempt to understand the mechanism of flash-sintering for the $MnCo_2O_4$ material. The major observations found in this work are as follows.

1. SEM images show dense grain growth by electric field (in addition to thermal) when local temperature is greater than 1050 °C. XRD analysis shows that the extent of new phase formation is more extensive in FS compared to CS samples treated to similar times. The phase decomposition and shrinkage occur concurrently in flash-sintering.
2. Systematic changes and close match of conductivities at higher temperature, where one is associated to purely thermal effect and the other dominantly by electric field, suggest sharing the same conductivity mechanism.

In case of flash-sintered FS925, FS975 and FS1050 samples, fast increase in conductivity produces avalanche of ionic-sites along with the increase in the specimen temperature due to the interaction of electric field. As the temperature in these cases is lower than 1080 °C, the material shows incompetence for the utilization of generated sites because of equally probable Co^{2+}–Co^{3+} transition. Hence, the microstructure is not improved (over CS) and stable-phase is observed in XRD spectra. For the samples FS1100, FS1160 and FS1320, an abrupt increase in the conductivity brings the specimen temperature to more than 1080 °C along with the generations of ionic-sites. As these temperatures are high enough, some of Co^{2+} states are stabilized increasing the life of O-site. Out of many oxygen sites, some result in the oxygen loss and some acts as site for diffusion. Faster sintering kinetics at temperatures in excess to 1100 °C causes ions/mass to utilize now-stable oxygen sites for diffusion and hence sintering occurs. A significantly dense microstructure produced at 1100 °C and 1160 °C supports such argument. From this study we conclude that the minimum temperature required for conventional sintering is above 1080 °C and we are able to attain the required conditions at 120–150 °C furnace temperature under the applied electric field of 15.0–17.5 V cm^{-1}.

6. Conclusions

In summary, we have demonstrated the flash-sintering of $MnCo_2O_4$ spinel at furnace temperature of 120–250 °C under the electrical field of 7.5–17.5 V cm^{-1} and current density of 1.40–1.60 A/mm^2. It has been shown that the furnace temperature, at which the flash-effect observes, can be reduced by increasing the density of the sample. We have also demonstrated that in flash-sintering power dissipation occurs at first, followed by Joule heating, which eventually leads to an increase in local specimen temperature. SEM analysis shows that the microstructure of the flash-sintered sample changes to dense and pore-free morphology at specimen temperature greater than 1080 °C. From XRD analysis, it is found that $MnCo_2O_4$ phase decomposes by significant amounts for samples treated to 1100 °C and higher temperatures. The concentration of secondary phase was found higher for flash sintered samples compared to that of conventionally sintered at the same time. Consistent changes in *I–V* behavior at different temperatures and close match of conductivities resulting from thermal and electric effect suggested that flash-effect is assisted by the mechanism of usual conductivity phenomenon. Correlating the microstructure, phase structure and conductivity, a mechanism of flash-sintering in $MnCo_2O_4$ spinel is proposed: the flash-sintering is accompanied through the natural ionic rearrangements, which occur during conductivity increase. Sintering is found to be drastically accelerated by utilizing these ionic sites when the specimen temperature is above 1080 °C. In addition, the work clarifies the extent of local temperature required for sintering which is important to know for the protective coating application.

Acknowledgments

The authors would like to thank Dr. Dario Montinaro from SOFCPower, Italy for providing raw materials for the work. Anshu Gaur would personally like to extend her thanks to him for the useful discussions.

References

1. Matsui K, Ohmichi N, Ohgai N. Sintering kinetics at constant rates of heating: effect of Al_2O_3 on the initial sintering stage of fine zirconia powder. *J Am Ceram Soc* 2005;**88**:3346–52.
2. Groza JR, Zavaliangos A. Sintering activation by external electrical field. *Mater Sci Eng A* 2000;**287**:171–7.

3. Chang-Jiang X, Zhen-Hua C. Ferroelectric behavior of 30 nm $BaTiO_3$ ceramics prepared by high pressure assisted sintering. *Chin Phys B* 2007;**16**:3125–8.
4. Marco Cologna M, Prette ALG, Raj R. Flash-sintering of cubic yttria-stabilized zirconia at 750 °C for possible use in SOFC manufacturing. *J Am Ceram Soc* 2011;**94**:316–9.
5. Cologna M, Francis JSC, Raj R. Field assisted and flash-sintering of alumina and its relationship to conductivity and MgO-doping. *J Eur Ceram Soc* 2011;**31**:2827–37.
6. Downs JA, Sglavo VM. Electric field assisted sintering of cubic zirconia at 390 °C. *J Am Ceram Soc* 2013;**96**:1342–4.
7. Raj R. Joule heating during flash-sintering. *J Am Ceram Soc* 2012;**32**:2293–301.
8. Karakuscu A, Cologna M, Yarotski D, Won J, Francis JSC, Raj R, et al. Defect structure of flash-sintered strontium titanate. *J Am Ceram Soc* 2012;**95**:2531–6.
9. Muccillo R, Muccillo ENS, Kleitz M. Densification and enhancement of the grain boundary conductivity of gadolinium-doped barium cerate by ultra fast flash grain welding. *J Eur Ceram Soc* 2012;**32**:2311–6.
10. Prette ALG, Cologna M, Sglavo VM, Raj R. Flash-sintering of Co_2MnO_4 spinel for solid oxide fuel cell applications. *J Power Sources* 2011;**196**:2061–5.
11. Hao X, Liu Y, Wang Z, Qiao J, Sun K. A novel sintering method to obtain fully dense gadolinia doped ceria by applying a direct current. *J Power Sources* 2012;**210**:86–91.
12. Zapata-Solvas E, Bonilla S, Wilshaw PR, Todd RI. Preliminary investigation of flash sintering of SiC. *J Eur Ceram Soc* 2013;**33**:2811–6.
13. Narayan J. A new mechanism for field-assisted processing and flash-sintering of materials. *Scr Mater* 2013;**69**:107–11.
14. Petric A, Ling H. Electrical conductivity and thermal expansion of spinels at elevated temperatures. *J Am Ceram Soc* 2007;**90**:1515–20.
15. Wang K, Liu Y, Fergus JW. Interactions between SOFC interconnect coating materials and chromia. *J Am Ceram Soc* 2011;**94**:4490–5.
16. Yang Z, Xia G, Stevenson JW. $Mn_{1.5}Co_{1.5}O_4$ spinel protection layers on ferritic stainless steels for SOFC interconnect applications. *Electrochem Solid State Lett* 2005;**8**:168–70.
17. Bentzen JJ, Høgh JVT, Barfod R, Hagen A. Chromium poisoning of LSM/YSZ and LSCF/CGO composite cathodes. *Fuel Cells* 2009;**9**:823–32.
18. Fergus JW. Effect of cathode and electrolyte transport properties on chromium poisoning in solid oxide fuel cells. *Int J Hydrogen Energy* 2007;**32**:3664–71.
19. Yi EJ, Yoon MY, Moon J, Hwang HJ. Fabrication of a $MnCo_2O_4$/gadolinia-doped ceria (GDC) dual-phase composite membrane for oxygen separation. *J Korean Ceram Soc* 2010;**47**:199–204.
20. Downs JA [PhD Thesis] *Mechanism of flash-sintering in zirconia*. Trento, Italy: University of Trento; 2013.
21. Bauerle JE. Study of solid electrolyte polarization by a complex admittance method. *J Phys Chem Solids* 1969;**30**:2657–70.
22. Kleitz M, Bernard H, Fernandez E, Schouler E. Impedance spectroscopy and electrical resistance measurements on stabilized zirconia. In: Heuer AH, Hobbs LW, editors. *Advances in ceramics: science and technology of zirconia*, vol. 3. Columbus, OH: The American Ceramic Society Inc.; 1981. p. 310.
23. Bergant Z, Grum J. Porosity evaluation of flame-sprayed and heat treated nickel-based coatings using image analysis. *Image Anal Stereol* 2011;**30**:53–62.
24. Francis JSC, Raj R. Influence of the field and the current limit on flash sintering at isothermal furnace temperatures. *J Am Ceram Soc* 2013;**96**:2754–8.
25. Mohiddon MA, Yadav KL. Reaction kinetics of PLZT formation and its effect on structural and dielectric properties. *Adv Appl Ceram* 2008;**107**:354–9.
26. Cullity BD. *Elements of X-ray diffraction*. London: Addition-Wesley Publishing Company; 1967. p. 99.
27. Lange F, Martin M. The electrical conductivity of CoO: experimental results and a new conductivity model. *Ber Bunsenges Phys Chem* 1997;**101**:176–84.
28. Massarotti V, Capsoni D, Bini M, Chiodelli G. Electric and magnetic properties of $LiMn_2O_4$- and Li_2MnO_3-type oxides. *J Solid State Chem* 1997;**131**:94–100.
29. Bordeneuve H, Rousset A, Tenailleau C, Guillemet-Fritsch S. Cation distribution in manganese cobaltite spinels $Co_{2-x}Mn_xO_4$ ($0 < x < 1$) determined by thermal analysis. *J Therm Anal Calorim* 2010;**101**:137–42.
30. Rajeevan NE, Kumar R, Shukla DK, Pradyumnan PP, Arora SK, Shvets IV. Structural, electrical and magnetic properties of bi-substituted Co_2MnO_4. *Mater Sci Eng B* 2009;**63**:48–56.
31. Hua B, Kong YH, Lu FS, Zhang JF, Pu J, Li J. The electrical property of $MnCo_2O_4$ and its application for SUS 430 metallic interconnect. *Chin Sci Bull* 2010;**55**:3831–7.